Heteroclinic tangles and homoclinic snaking in the unfolding of a degenerate reversible Hamiltonian Hopf bifurcation

P.D. Woods & A.R. Champneys*
Department of Engineering Mathematics, University of Bristol, UK.

July 7, 1998

Abstract

This paper considers an unfolding of a degenerate reversible 1−1 resonance (or Hamiltonian Hopf) bifurcation for four-dimensional systems of time-reversible ordinary differential equations (ODEs). This bifurcation occurs when a complex quadruple of eigenvalues of an equilibrium coalesce on the imaginary axis to become two imaginary pairs. The degeneracy occurs via the vanishing of a normal form coefficient ($q_2 = 0$) that determines whether the bifurcation is super- or sub-critical. Of particular concern is the behaviour of homoclinic and heteroclinic connections between the trivial equilibrium and simple periodic orbits. A partial unfolding of such solutions already occurs in the work of Dias & Iooss (*Eur.J.Mech.B-Fluids* **15** (1996) 367-393), given a sign of the coefficient of a higher-order term ($q_4 < 0$). Here, their analysis is generalised to include the other sign of q_4, motivated by a fourth-order ODE whose solutions model localised buckling of struts and steady states of the generalised Swift-Hohenberg equation.

Numerical experiments are undertaken to determine the global behaviour of homoclinic orbits to the origin in the example, which is both reversible and Hamiltonian. The normal form coefficients are calculated explicitly and a region of parameter space found where $q_4 > 0$ and $-1 \ll q_2 < 0$. The normal form then shows a small-amplitude bifurcating branch of homoclinic solutions terminating at a heteroclinic connection to a simple periodic orbit. A genericity argument shows that this connection is not structurally stable and should break into a pair of heteroclinic tangencies. This is confirmed by numerics which shows that branches of the simplest homoclinic orbits undergo an infinite snaking sequence of limit points accumulating on the parameter values of the two tangencies. At each limit point the homoclinic orbit generates another 'bump' close to the periodic. As q_2 is further decreased from zero, the snake widens until, at a critical value, a branch is formed of heteroclinic connections from the origin to a non-trivial equilibrium (a 'kink'). For q_2 less than this value the kinks, heteroclinic tangencies and snake-like curves no longer occur.

1 Introduction

In this paper we consider four-dimensional smooth systems of ordinary differential equations

$$\dot{x} = f(x, \mu) \quad x \in \mathbb{R}^4, \quad \mu \in \mathbb{R}^p, \tag{1}$$

which are reversible in the sense that there is a linear transformation R that fixes half the phase-space variables (Devaney 1976*b*, Lamb & Roberts 1998)

$$\exists R, \quad R^2 = \mathrm{Id}, \quad \mathcal{S} = \mathrm{fix}(R) \cong \mathbb{R}^2, \quad Rf(x, \mu) = -f(Rx, \mu). \tag{2}$$

Here $\mathcal{S}$ is termed the *symmetric section* of the reversibility and orbits of (1) that intersect $\mathcal{S}$ are referred to as being *symmetric* under R. An important class of reversible systems are ones that can be written (perhaps under a change of co-ordinates) in Hamiltonian form $\dot{y} = J\nabla H(y)$, where J is the

*author to whom correspondence should be addressed

usual skew-symmetric matrix in $\mathbb{R}^4$. The local bifurcation we have in mind (four complex eigenvalues becoming pure imaginary as a parameter μ passes through zero, see Figure 1) requires only reversible structure, not necessarily Hamiltonian. Despite this we shall refer to such a 1-parameter bifurcation as a Hamiltonian-Hopf, although it has also attracted the names 'reversible $1-1$ resonance' and 'reversible Hopf bifurcation' in the literature.

For a good general reference on Hamiltonian-Hopf bifurcations see the monograph by van der Meer (1985). Our main concern will be the small amplitude bifurcation of localised (homoclinic-to-zero) solutions at Hamiltonian Hopf bifurcations, because of their importance in describing solitary travelling waves or finite energy deformations of spatial problems on the real line (see, for example, Champneys (1998) and references therein). Iooss & Pérouème (1993) describe rigorously an unfolding of homoclinic orbits born in reversible Hamiltonian Hopf bifurcations. They show that for a certain sign of a co-efficient of the normal form ($q_2 < 0$) there is the subcritical ($\mu < 0$) bifurcation of a pair of reversible homoclinic orbits. In fact, the situation is more subtle because, consequent on the complex eigenvalues for $\mu < 0$, generically there should be infinite families of homoclinic orbits which are like 'multi-pulsed' versions of the two bifurcating primaries (Härterich 1998).

Here we are interested in the codimension-two bifurcation that occurs when q_2 passes through zero. This has already been partially analysed by Dias & Iooss (1996) under a condition on the sign of a higher-order term ($q_4 < 0$) that was motivated by a problem in interfacial water waves. They found heuristically a rich family of periodic, quasi-periodic and localised solutions including homoclinic connections to periodic orbits that resemble dark envelope soliton solutions of Nonlinear Shrödinger (NLS) type equations. Also Iooss (1997) has proved rigorously that certain algebraically decaying finite-amplitude homoclinic solutions, which exist for a truncated normal form for $\mu = 0$ and $1 \gg q_2 > 0$ and $q_4 < 0$, actually persist beyond terms that break the normal form structure.

In this paper we complete the heuristic unfolding of the degenerate reversible Hamiltonian-Hopf bifurcation by considering all possible sign combinations of the appropriate nonlinear terms of the truncated normal form. We shall not attempt to prove rigorous persistence results Instead we shall indicate via numerical calculations on an example system, both the accuracy of our analysis and and its weaknesses in unfolding a certain heteroclinic connection between an equilibrium and a periodic orbit. The numerics will show a rich bifurcation structure (a 'homoclinic snake') caused by the unfolding of this connection into a *heteroclinic tangle*. We shall also show, at least for this one example, the mechanism by which this snake is destroyed upon moving parameters far away from the Hamiltonian-Hopf.

Underlying our study we have in mind the canonical fourth-order example equation

$$u_{tttt} + Pu_{tt} + g(u) = 0, \quad \text{where} \quad g(u) = u - au^2 + bu^3, \quad (a, b > 0). \tag{3}$$

Under the change of co-ordinates, e.g.

$$q_1 = u, \quad q_2 = u_{tt} + \frac{P+2}{2}u, \quad p_1 = \frac{P-2}{2}u_t + u_{ttt}, \quad p_2 = u_t,$$

(3) is equivalent to a two degree-of-freedom Hamiltonian dynamical system with energy

$$H = u_t u_{ttt} + \frac{P}{2}u_t^2 - \frac{1}{2}u_{tt}^2 + G(u), \quad \text{where} \quad G(u) = \int_0^u g(v)\, dv. \tag{4}$$

This dynamical system is also reversible in the sense of (2); specifically (3) is invariant under

$$R : (u_t, u_{ttt}) \to (-u_t, -u_{ttt}) \quad \text{and} \quad t \to -t. \tag{5}$$

Finally, note that equilibria are given by

$$u = 0, \quad \text{or (if } b > a/4) \quad 1 - au + bu^2 = 0. \tag{6}$$

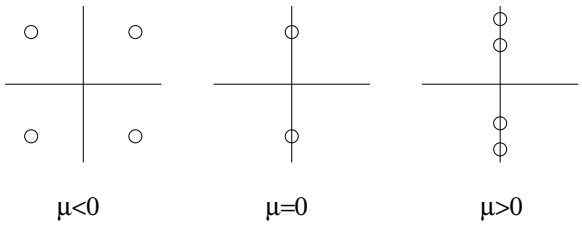

Figure 1: The behavior of eigenvalues at a Hamiltonian-Hopf bifurcation

In Section 6 below we shall show that this system undergoes a degenerate Hamiltonian-Hopf bifurcation at the origin for $P = 2$ and $b = 38a/27$, whereupon it satisfies $q_4 > 0$, the opposite case to that analysed by (Dias & Iooss 1996).

Equation (3) arises in several contexts. First (Hunt, Bolt & Thompson 1989, Hunt & Wadee 1991, Hunt, Woods, Champneys, Peletier, Wadee & Budd 1998) it represents the dimensionless equilibrium equation of an elastic strut of deflection u with respect to an infinite spatial co-ordinate t running along its length. Here P is the strength of a compressive load and $g(u)$ models the effect of a foundation with destiffening and re-stiffening nonlinearities. In that case, for long struts, the solutions of interest are homoclinic to zero, i.e. $u(t) \to 0$ as $t \to \pm\infty$. A second scaling of (3) arises as the steady state equation for the generalised Swift-Hohenberg equation (Glebsky & Lerman 1995, Hilali, Métens, Borckmans & Dewel n.d.) where there is interest in phase transitions modelled by homoclinic and heteroclinic connections among the origin and the nontrivial equilibria (6).

See Champneys (1998) for a review of other applications of (3) for various $g(u)$, including (with $g = u^2$) its derivation as a rigorous centre-manifold reduction for capillary-gravity water waves with near-critical Bond and Froude numbers (Iooss & Kirchgässner 1990, Buffoni, Groves & Toland 1996). The behaviour of homoclinic solutions to (3) when $b = 0$ is now almost completely understood (Buffoni, Champneys & Toland 1996, Buffoni & Séré 1996, Champneys 1998). Here we shall focus on the extra features that occur for $b > 0$.

The rest of the paper is outlined as follows. In Section 2, we shall recall the truncated normal form of the Hamiltonian-Hopf bifurcation and its reduction (Iooss & Pérouème 1993) to a second-order nonlinear oscillator. Sections 3 and 4 then analyses solutions to this oscillator equation by examining carefully graphs of its potential energy. Particular attention is paid to the existence of homoclinic and heteroclinic trajectories. Section 5 discusses questions of persistence of solutions with the addition of terms that break the completely integral normal form structure. Section 6 then presents the results of numerical experiments on equation (3). Finally, Section 7 draws conclusions, suggests future analyses and highlights possible implications of the results for localised buckling and pattern formation problems.

2 Normal form

The Hamiltonian-Hopf bifurcation of a symmetric equilibrium of a reversible system occurs when two symmetric pairs of complex conjugate eigenvalues of the linearisation coalesce and form two pairs of imaginary eigenvalues as shown in Figure 1. Here μ is the parameter that unfolds the bifurcation.

The normal form for the Hamiltonian-Hopf bifurcation is (Elphick, Tirapegui, Brachet, Coullet & Iooss 1987, Iooss & Pérouème 1993, Dias & Iooss 1996)

$$\frac{dA}{dt} = i\omega A + B + iA\,P\left(\mu; |A|^2, \frac{i}{2}(A\bar{B} - \bar{A}B)\right) + R_A \tag{7}$$

$$\frac{dB}{dt} = i\omega B + iB\,P\left(\mu; |A|^2, \frac{i}{2}(A\bar{B} - \bar{A}B)\right) + A\,Q\left(\mu; |A|^2, \frac{i}{2}(A\bar{B} - \bar{A}B)\right) + R_B \tag{8}$$

where P and Q are polynomials with real coefficients which to lowest order take the form

$$P(\mu; x, y) = p_1\mu + p_2 x + p_3 y, \quad Q(\mu; x, y) = -q_1\mu + q_2 x + q_3 y + q_4 x^2, \tag{9}$$

and R_A and R_B are terms of higher order. In what follows, the coefficients of P are unimportant and q_3 plays a subservient role. We assume that the bifurcation occurs in the way illustrated in Figure 1, consequentially we may take $q_1 > 0$. Following Iooss and Peroueme we shall refer to the bifurcation on varying μ as being sub or super-critical depending on whether $q_2 < 0$ or $q_2 > 0$ respectively.

Generically it is unnecessary to include q_4 in an analysis of the bifurcation (Iooss & Pérouème 1993), unless q_2 is small (Dias & Iooss 1996) which is precisely the situation that interests us. Therefore, we shall regard μ and q_2 as independent small parameters unfolding the codimension two point where they are both zero. A scaling argument in Dias & Iooss (1996) shows that if

$$q_2 = \varepsilon, \quad \text{and} \quad A = \mathcal{O}(\sqrt{\varepsilon}), \quad B = \mathcal{O}(\varepsilon\sqrt{\varepsilon}), \quad t = \mathcal{O}(\sqrt{\varepsilon}), \quad \mu = \mathcal{O}(\varepsilon^2),$$

then the ignored terms in the normal form upon taking $R_A = R_B = 0$ and (9) are consistently of higher-order in ε. Therefore, at least formally, to lowest order in ε the assumed forms of P and Q are sufficient to unfold the codimension-two bifurcation.

The system (7),(8) with $R_A = R_B = 0$ is completely integrable with integrals K and H defined by

$$\begin{aligned} K(\mu, A, B) &= \frac{i}{2}(A\overline{B} - \overline{A}B) \\ H(\mu, |A|^2, |B|^2, i/2K) &= |B|^2 - \int_0^{|A|^2} Q(\mu, s, K)ds. \end{aligned}$$

Using these integrals it is straightforward to write the system as a single nonlinear oscillator equation for $x = |A|^2$. Note that choosing such a co-ordinate in effect factors out the fast dynamics which are terms in A proportional to $e^{i\omega}$. Specifically, from (7) without remainder terms we have $\frac{dx}{dt} = A\overline{B} + B\overline{A}$, and hence

$$\left(\frac{dx}{dt}\right)^2 = 4x\left(H + \int_0^x Q(\mu, s, K)ds\right) - 4K^2 := 4f(x). \tag{10}$$

This equation may be viewed as the expression for conservation of zero total energy of a particle of unit mass and position x confined to lie in a potential well, with potential $-4f(x)$. Taking the approximations (9), the function f is of the form

$$f(x : \mu, H, K) = \frac{1}{3}q_4 x^4 + \frac{1}{2}q_2 x^3 + (q_3 K - q_1\mu)x^2 + Hx - K^2. \tag{11}$$

To understand the dynamics near the codimension two point we shall study the roots of the negative of the potential $f(x)$ for μ and q_2 small.

Equivalently, upon differentiating with respect to t, (10) can be expressed as a nonlinear oscillator equation for x_{tt} in terms of x Then, from the given form of f, one could attempt to read off explicit solutions at certain parameter values (such as homoclinic orbits in terms of hyperbolic secant functions). Rather than adopting such an analytic approach, we shall rely on a geometric approach, since the shape of shape of f entirely determines the dynamics of (10).

Now, since x is real, solutions to (10) only make sense if $f \geq 0$. Also, since $x = |A|^2$, we are only interested in solutions for $x > 0$. Our primary concern will be with homoclinic orbits, these are represented by a particle which starts at rest at a double root x^* of of f (corresponding to an equilibrium of (10)) and then passes upwards until another root is encountered at which point it must return backwards along the same path. Thus, for orbits homoclinic to an equilibrium $x = x^*$, there are conditions on the shape of $f(x)$:

- $f(x)$ must become positive on one side of $x = x^*$ (so x^* cannot be a local maximum of f); also if x^* is the origin, then we must have $f(x) > 0$ for all $x < a$ for some $a > 0$.

- If $f(x)$ locally increases for one sign of $x - x^*$, then for a homoclinic orbit to exist there must be a non-negative root bounding this region of positive f.

We should stress the relation between homoclinic orbits of the reduced oscillator equation (10) and the truncated normal form (7), (8) with $R_A = R_B = 0$ and P and Q given by (9). (10) is the equation for the square amplitude of A. Similar equations can easily be derived for the phase of A and the amplitude and phase of B (Iooss & Pérouème 1993, Eq. (9)). The leading order terms of these three equations just give rotation corresponding to the imaginary eigenvalues $\pm i\omega$. All other terms are slaved to (10) in that the right-hand sides depend only on μ, $x = |A|^2$ and the integrals H and K. The form of these equations implies that solutions to (10) correspond to one-parameter family of solutions of the full system parametrised by shifts in phase $(A, B) \to (Ae^{i\phi}, Be^{i\phi})$. Also, non-trivial equilibria of (10) correspond to periodic orbits of the normal form. Hence a homoclinic orbit to the origin of the amplitude equation (10) corresponds to a one-parameter family of homoclinic solutions to the origin of (7),(8), whereas a homoclinic orbit to a non-trivial equilibrium corresponds to a one-parameter family of homoclinic connections to a periodic orbit in the normal form equations.

It is a much more delicate question to determine persistence of solutions under the inclusion of higher-order terms $R_A, R_B \neq 0$ which break the completely integrable structure of the normal form. We shall return to this question in Section 5 below. In the meantime we note that the origin $(A, B) = (0, 0)$ satisfies $H = K = 0$ so homoclinic solutions to the origin, 'bright solitons' in the parlance of NLS-type equations, must lie in these zero energy surfaces. We treat this special case first in Section 3 that follows. After that we treat general values of H and K and look for possible homoclinic connections to non-trivial equilibria. Such homoclinic connections to periodic orbits have been given the name 'dark solitons' (see, e.g. Dias & Iooss (1996)). We shall refer to *bright* homoclinic solutions as those whose x-value at their mid-point is higher than the x-value to which they asymptote and *dark* homoclinic solutions as those obeying the reverse.

3 Homoclinic orbits in the zero energy surface

We start our analysis by considering (11) with $H = K = 0$,

$$\left(\frac{dx}{dt}\right)^2 = 4f(x), \quad \text{where} \quad f(x) = \frac{q_4}{3}x^4 + \frac{q_2}{2}x^3 - q_1\mu x^2. \tag{12}$$

The dynamics of (12) and hence the existence or otherwise of homoclinic orbits is crucially dependent on the sign of q_4. The two cases are treated separately.

3.1 q_4 positive

First, dividing out the double root of f at the origin leaves a quadratic in x

$$g(x) \quad = \quad \frac{q_4}{3}x^2 + \frac{q_2}{2}x - q_1\mu,$$

an expression for whose roots is

$$x_{1,2} = \frac{3}{2q_4}\left(-\frac{q_2}{2} \pm \sqrt{D_g}\right), \quad \text{where} \quad D_g = \frac{q_2^2}{4} + \frac{4q_1q_4\mu}{3}. \tag{13}$$

Using equation (13) consider the effect of varying μ and q_2. The results are summarised in Figure 2. First note that D_g is always positive for μ positive, but that it can be negative for negative μ. If $\mu > 0$ then $|D_g| \geq |\frac{q_2^2}{4}|$, so $g(x)$ has one positive and one negative root. Returning to $f(x)$, one can see that the double root at the origin flanked by roots on either side must be a local maximum. This means there are no homoclinic orbits for $\mu > 0$.

However, if $\mu < 0$ then $g(x)$ has either two positive or two negative roots, depending on the sign of q_2. Looking at the graph of $f(x)$, one can see that the case of a double root at the origin with two positive roots ($q_2 < 0$) is such that there is a homoclinic orbit to the origin, whereas the case with two negative roots cannot support homoclinic orbits.

So the region of existence of homoclinic-to-zero solitons is $\mu < 0$, $q_2 < 0$ and $D_g < 0$. This region has two boundaries: where $\mu = 0$ and where $D_g = 0$, i.e.

$$\mu = \mu_D := \frac{-3q_2^2}{16q_1q_4}.$$

When the homoclinic orbit approaches the first of these, its amplitude goes to zero. The scaling of these homoclinic solutions as $\mu \to 0^-$, assuming q_2 is not small is easily calculated (see also Iooss & Pérouème (1993)). The smaller of the two roots of g

$$x_1 = \frac{3}{2q_4}\left(-\frac{q_2}{2} - \sqrt{D_g}\right) \quad = \frac{-2q_1\mu}{q_2} + \mathcal{O}(\mu^2),$$

gives the maximum amplitude of homoclinic orbit. Now to calculate the amplitude of the homoclinic orbit for the normal form (7), (8) we use the fact that $|A| = \sqrt{|x|} = \mathcal{O}(\sqrt{\mu})$. Also, using $H = 0$ we have

$$|B| = \sqrt{-q_1\mu|A|^2 + q_2|A|^2} = \mathcal{O}(\mu).$$

So the one-parameter family of homoclinic solutions looks like

$$A(t) = \mathcal{O}(\sqrt{\mu})\exp(i\omega t + \phi), \quad B(t) = \mathcal{O}(\mu)\exp(i\omega t + \phi), \tag{14}$$

for arbitrary initial phases $0 \le \phi < 2\pi$.

At the other boundary of the region of existence of homoclinic solutions there is a double root of g at $x = -3q_2/4q_4$, which corresponds in the full normal form (7), (8) to a finite-amplitude periodic orbit. Hence the homoclinic orbit to the origin has become a heteroclinic connection between the origin and this periodic orbit. The existence of this heteroclinic orbit will play a crucial role in the numerical experiments in Section 6 below. (Note that the other branch of the curve $D_g = 0$ has no meaning since the double root occurs for $x < 0$).

Thus there are four open parameter regions in the (μ, q_2)-plane corresponding to qualitatively distinct dynamics, as shown in Figure 2. The region numbers in the figure are the same as in the summary below.

1. When $\mu > 0$ the graph of $f(x)$ has a negative root, a double root at the origin and a positive root. The fact that the double root is a maximum precludes the existence of homoclinic orbits of (10) since f is negative locally.

2. When $0 > \mu > \mu_D$ and $q_2 < 0$, then $f(x)$ has a double root at the origin and two positive roots. Since the double root is a local minimum, there are homoclinic orbits, the maximum amplitude of which are given by the first positive root.

3. When $\mu = \mu_D$ and $q_2 < 0$ there is a double root at $x = 0$ and also at $x = -\frac{3q_2}{4q_4}$. This means that on this half-parabola there is a heteroclinic connection (see above).

4. When $\mu < \mu_D$ there are no zeros of f other than the double root at the origin.

5. When $0 > \mu > \mu_D$ and $q_2 > 0$, the two non-trivial roots of $f(x)$ are negative and so there can be no homoclinic orbits for $x > 0$.

We have focussed on the possible existence of homoclinic solutions, but from the shapes of the graphs of f illustrated in the insets to Figure 2, the reader may also infer information about periodic and quasi-periodic solutions with $H = K = 0$.

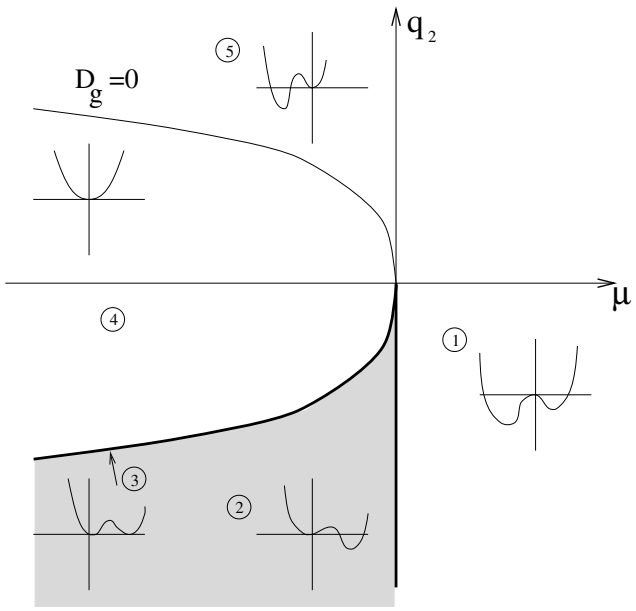

Figure 2: Summary of the behavior for $q_4 > 0$. The insets show graphs of $f(x)$, and the shading represents the region of existence of homoclinic orbits to the origin. Numbered regions are explained in the text.

3.2 q_4 negative

This case has been analysed in (Dias & Iooss 1996, Iooss 1997). For completeness, we list here the results which may be obtained using the same methods as the previous subsection. The numbered sections below refer to the numerically labeled open parameter regions and special curves numbered in Figure 3.

1. On the line $\mu = 0, q_2 > 0$ there is a triple root at the origin and a positive root with f positive in between. Such a graph represents a homoclinic orbit to a degenerate equilibrium at the origin. We note that such a solution decays algebraically to zero (for more details see (Iooss 1997)).

2. In the region $\mu < 0$ in addition to a local minimum of f at the origin, there is a positive and a negative root. Hence there is a homoclinic orbit. Note that, in contrast to the case where $q_4 > 0$ there are homoclinic orbits to the origin for both subcritical ($q_2 < 0$) *and* supercritical ($q_2 > 0$) bifurcations. The distinction between the two cases, is that on decreasing μ from zero, the homoclinic orbits bifurcate from small amplitude for $q_2 < 0$, but from finite-amplitude algebraically decaying solutions when $q_2 > 0$. In particular, for $q_2 < 0$ the scalings (14) hold, whereas for $q_2 > 0$, the amplitude of the homoclinic is finite at $\mu = 0$. At the transition between super- and sub-criticality, $q_2 = 0$ we have

$$A(t) = \mathcal{O}(\sqrt[4]{\mu}) \exp(i\omega t + \phi), \quad B(t) = \mathcal{O}(\mu^{3/4}) \exp(i\omega t + \phi). \tag{15}$$

3. On the line $\mu = 0, q_2 < 0$ there is a triple root at the origin and a negative root. There are no homoclinic orbits.

4. In the region $0 < \mu < \mu_D$,$q_2 < 0$ there is a double root at the origin and two negative roots.

5. In the region $0 < \mu_D < \mu$ there is only the double root at the origin.

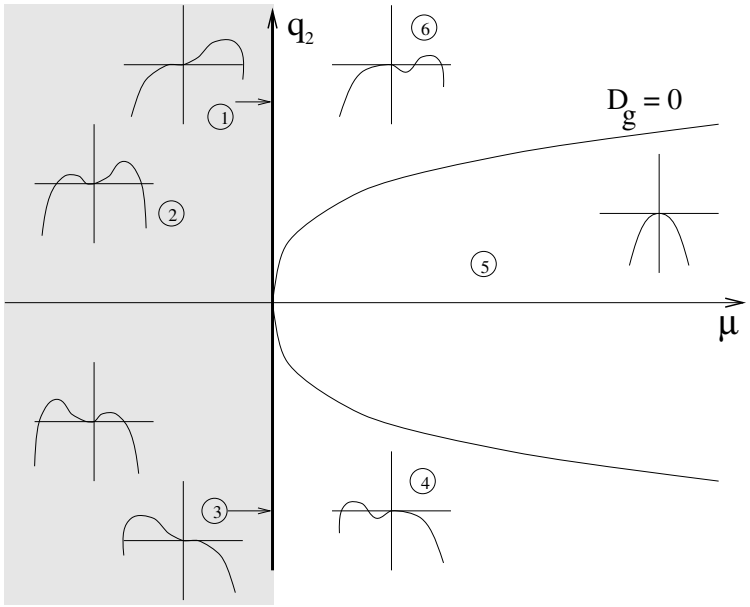

Figure 3: Analogous to figure 2 but for $q_4 < 0$.

6. In the region $0 < \mu < \mu_D, q_2 > 0$ there is a minimum at the origin and two positive roots. Hence there are no homoclinic orbits.

In summary, there are exponentially-decaying homoclinic orbits for all $\mu < 0$ and algebraically decaying homoclinic orbits for $\mu = 0, q_2 > 0$.

4 Homoclinic orbits in non-zero energy surfaces

Dias & Iooss (1996) showed the existence of various kinds of homoclinic-to-periodic solutions of (10) for $(H, K) \neq (0, 0)$ in the case $q_2 > 0$, $q_4 < 0$. We shall repeat their analysis technique and extend it to cover all possible combinations of signs of q_2 and q_4. We shall also consider the special case that arises when q_3 is taken to be zero.

As the normal form motivates this investigation, only $x > 0$ and $f(x) > 0$ are considered. We start by looking at conditions for multiple roots of f, which in general represent periodic solutions of (7), (8) and may represent the end points of homoclinic solutions.

4.1 Conditions for multiple roots of f

For double roots we require

$$f(x; H, K, \mu) = \frac{1}{3}q_4x^4 + \frac{1}{2}q_2x^3 - (q_1\mu - q_3K)x^2 + Hx - K^2 = 0\,, \tag{16}$$

$$\frac{df}{dx}(x; H, K, \mu) = \frac{4}{3}q_4x^3 + \frac{3}{2}q_2x^2 - 2(q_1\mu - q_3K)x + H = 0\,, \tag{17}$$

One can eliminate H between these equations, which gives a quadratic

$$K^2 + q_3x^2K + q_4x^4 + q_2x^3 - q_1\mu x^2 = 0\,, \tag{18}$$

that can be solved for K if its discriminant Δ is positive:

$$\Delta = x^2((q_3^2 - 4q_4)x^2 - 4q_2x + 4q_1\mu) \geq 0\,. \tag{19}$$

We denote by μ_m the value of μ that makes the discriminant of the non-trivial quadratic factor of (19) vanish, its value is

$$\mu_m = \frac{q_2^2}{q_1(q_3^2 - 4q_4)}\,, \quad x_m = \frac{2q_2}{q_3^2 - 4q_4}\,. \tag{20}$$

For $\mu > \mu_m$, Δ is positive for all values of x. Hence, for each value of x there are two values of K (and consequently H) solving (16),(17)

$$K_\pm = \frac{1}{2}(-q_3x^2 \pm \sqrt{\Delta}), \quad H_\pm = -\frac{4}{3}q_4x^3 - \frac{3}{2}q_4x^2 + 2(q_1\mu - q_3K_\pm)x.$$

Note that K_+ is zero when $-4q_4x^2 - 4q_2x + 4q_1 = 0$, whereas K_- is never zero except at $x = 0$.

The boundary in the (x, μ)-plane of existence of double roots of (18) is given by $\Delta = 0$, i.e.

$$D = \left\{ (x,\mu) : x = x_\pm := \frac{2q_2 \pm 2\sqrt{-q_2^2 - q_1\mu(q_3^2 - 4q_4)}}{q_3^2 - 4q_4} \right\}. \tag{21}$$

On D, there is only one K-value giving a solution.

We now look for triple roots. They can be obtained by setting $f(x)$ and its first two derivatives equal to zero. This leads to the following expressions,

$$K_\pm^t = \pm\sqrt{q_4x^4 + \frac{1}{2}q_2x^3}, \qquad H_\pm^t = \frac{8}{3}q_4x^3 + \frac{3}{2}q_2x^2\,, \tag{22}$$

$$q_1\mu_\pm^t = \pm q_3\sqrt{q_4x^4 + \frac{1}{2}q_2x^3} + 2q_4x^2 + \frac{3}{2}q_2x\,, \tag{23}$$

These conditions define a curve T of triple roots in the (x, μ) plane. Setting the third derivative equal to zero also gives an expression for quadruple roots, namely that in addition to (22) and (23) we have

$$x = x^q := \frac{-3q_2}{8q_4}\,.$$

So quadruple roots occur at isolated points Q in the (x, μ) plane, which, since x must be positive in (10), are only meaningful when q_4 and q_2 have opposite signs.

In what follows we shall view regions in the (x, μ)-plane corresponding to differing numbers of multiple roots upon varying K. We shall also infer information on the existence of homoclinic orbits from the location of these roots in x, and from the shape of the graph of $f(x; H, K, \mu)$. As in Section 3, we leave it to the reader to glean information from the various graphs about existence of periodic and quasi-periodic solutions.

4.2 q_4 negative

4.2.1 Supercritical bifurcation: $q_2 > 0$

If we set $q_4 < 0$ and $q_2 > 0$ in equation (21) then D has a maximum with respect to μ at

$$M: \quad (x_m, \mu_m) = \left(\frac{4}{5}, \frac{4}{5}\right). \tag{24}$$

So for $\mu > \mu_m$ there are two surfaces of solutions to (18) for each value of μ; while for $0 < \mu < \mu_m$ there are four, two each side of D. See Figure 4. Along D, K_+ and K_- merge smoothly in a fold.

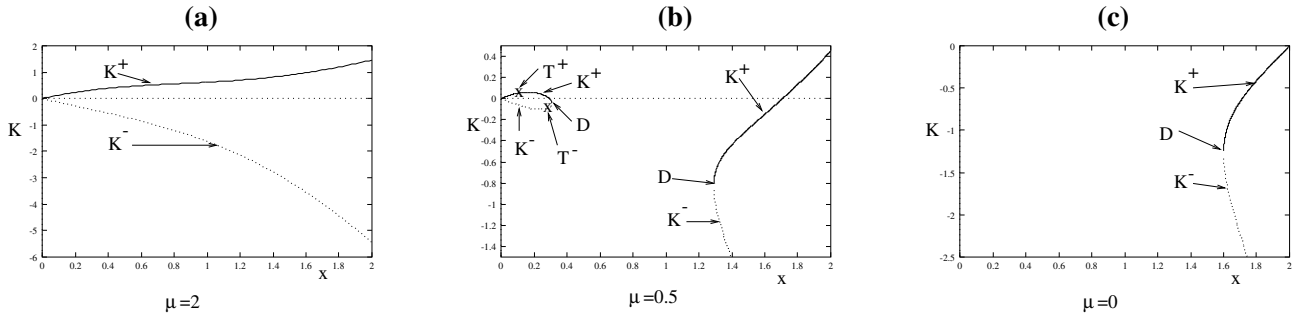

Figure 4: Curves of solutions to (18) in the (x, K)-plane for (a) $\mu = 2 > \mu_m = \frac{4}{5}$, (b) $\mu = 1/2 < \mu_m$, (c) $\mu = 0 < \mu_m$ for $q_4 < 0$, $q_2 > 0$. $(q_4 = -1, q_3 = 1, q_2 = 2, q_1 = 1)$

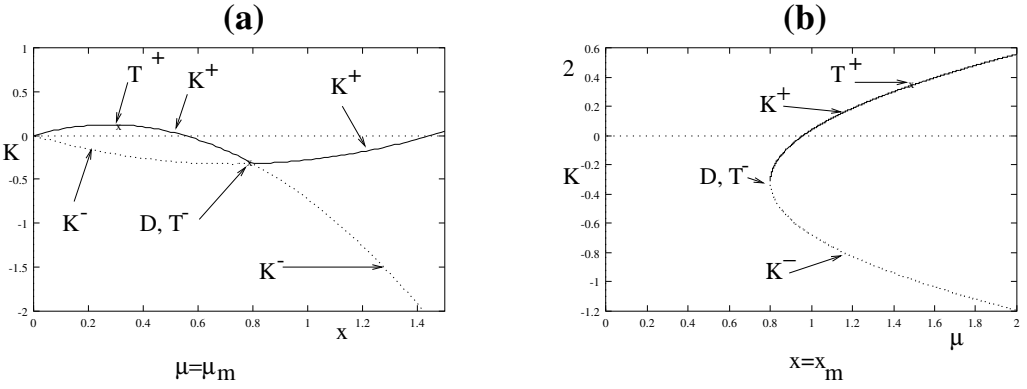

Figure 5: The $x - K$ and $\mu - K$ planes for $\mu = \mu_m = \frac{4}{5}$ and $x = x_m = \frac{4}{5}$ for $q_4 < 0$, $q_2 > 0$ $(q_4 = -1, q_3 = 1, q_2 = 2, q_1 = 1)$

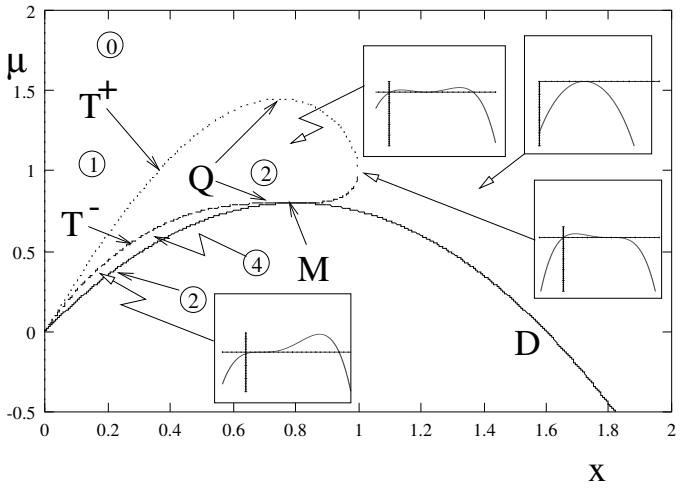

Figure 6: Projections of degenerate curves and points onto the (x, μ)-plane for $q_4 < 0$, $q_2 > 0$ and $q_3 \neq 0$. See text for details.

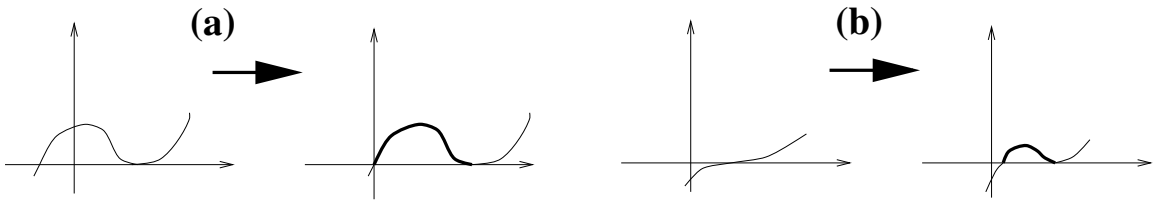

Figure 7: Creating homoclinic orbits by varying μ. Depicted are graphs of $f(x)$, the bold portions of which correspond to homoclinic orbits.

Hence at x_m all four solution surfaces are pinched together; see Figure 5. For $\mu < 0$ there are only two sets of solutions (for $x > x_+$) because x_- becomes negative. Sheets of solutions join at D.

There are also triple roots, given by putting $q_4 < 0$, $q_2 > 0$ in equations (22) and (23). On this curve, T, there are two K-values, K_+^t and K_-^t with corresponding μ-values μ_+^t and μ_-^t. T is a closed curve because the square-rooted quantity in equations (22) and (23) is undefined for $x > q_2/2q_4$.

Figure 6(a) shows the curves D, T_+ and T_-, and points Q and M projected onto the (x, μ)-plane. In this and subsequent similar figures, numbers in circles attached to regions, curves or points refer to the number of homoclinic orbits that occur (possibly in different sheets in the (K, x)-plane) at those (x, μ)-values. By the x-value of a homoclinic orbit we mean the value of x at the equilibrium or periodic orbit (double root of f) that the solution is asymptotic to. Some representative graphs of the $f(x)$ are also given as inserts in the figure.

We now know about what types of double roots of f there are for $q_4 < 0$, $q_2 > 0$: double roots everywhere outside the region bounded by the curve D of the discriminant being zero, and isolated curves of triple roots. Now we try to locate all possible homoclinic solutions. First note that there are two ways homoclinic orbits can be created as the parameter μ is varied (see Figure 7). One notes that the first method involves a positive y-intercept of f, this is prohibited by the form of equation (16). So there have to be triple roots for there to be the creation of homoclinic orbits. Thus it is important to note from the figures how T interacts with K_+ and K_-.

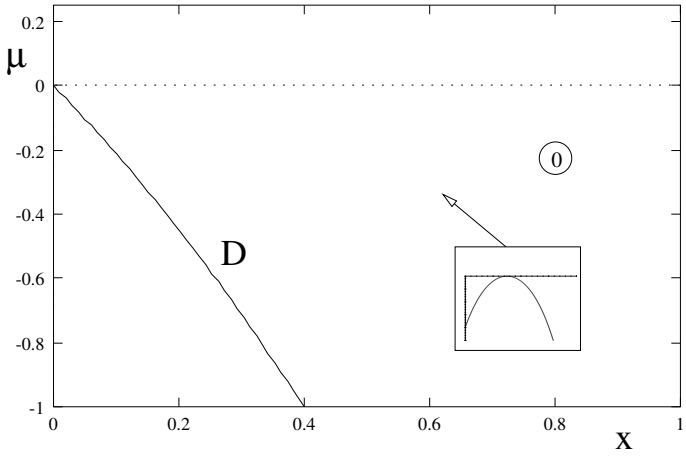

Figure 8: Projections of degenerate curves and points onto the (x, μ)-plane for $q_4 < 0$, $q_2 < 0$ and $q_3 \neq 0$. See text for details.

In K^+, $f(x)$ admits a pair of homoclinic orbits in the region in Figure 6(a) bounded by T^+ and D. Similarly, in K^-, $f(x)$ admits a pair of homoclinic orbits in the region of Figure 6(a) bounded by T^- and D. At $T^\pm$ in both cases, there are algebraically decaying bright homoclinic orbits except in the region of T between the two quadruple root points Q. In this latter region T represents algebraically decaying dark homoclinic orbits. Figure 5 shows the process by which T changes K-sheets at M.

4.2.2 Subcritical bifurcation: $q_2 < 0$

If $q_2 < 0$ while $q_4 < 0$ in equation (21), then the boundary D ($\Delta = 0$), of double roots has a maximum in μ at $(x_m, \mu_m) = (-4/5, 4/5)$ where x_m and μ_m are given by (24) A typical (x, K) projections looks like graph Figure 4(c). The boundary D goes through the origin in the $x_\pm, \mu$ plane, see Figure 8(a). T consists of one point, the origin (a negative triple root). The lack of non-trivial triple roots means there are no homoclinic orbits unless $q_3 = 0$ (see Figure 4(b)).

4.3 q_4 positive

Now we move on to the case not analyzed by Dias & Iooss (1996), but which has relevance to the example (3). If $q_4 > 0$, then the sign of $4q_4 - q_3^2$ is important. So, taking either sign of q_2, there are four sub-cases.

4.3.1 $4q_4 > q_3^2$, supercritical

If $4q_4 > q_3^2$ and $q_2 > 0$ then D ($\Delta = 0$) has a minimum in μ at zero. Double roots exist for $0 < x < x_+$. D is a parabola that points up rather than down in the (x, μ)-plane (as was the case for $q_4 < 0$) and passes through the origin. There are two sheets of double roots $K_\pm$. A typical graph of solutions in the (x, K)-plane would look like Figure 11(a) (even though that was computed for $q_2 < 0$). T^+ lies in K_+ and T^- in K_-. T is defined for all $x > 0$. The square-rooted quantity in equations (22) and (23) has no positive roots, so that T is unbounded in the (x, μ) plane. Figure 9(a) depicts the general situation. Note that the curve of triple roots no longer represents algebraically decaying homoclinic orbits when $q_4 > 0$, because of the shape of the associated potential. The root other than the triple root is negative and so is not important in the normal form. However T retains its importance in the creation of homoclinic orbits

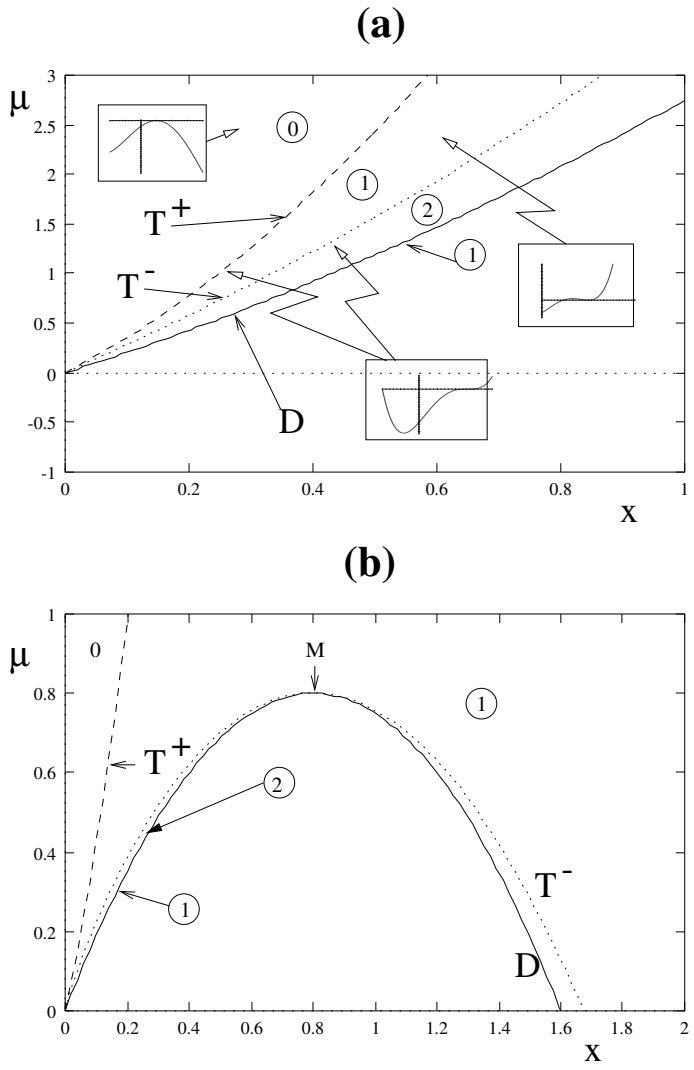

Figure 9: Projections of degenerate curves and points onto the (x, μ)-plane for $q_4 > 0$, $q_2 > 0$ and (a) $q_3^2 < 4q_4$, (b) $q_3^2 > 4q_4$. See text for details

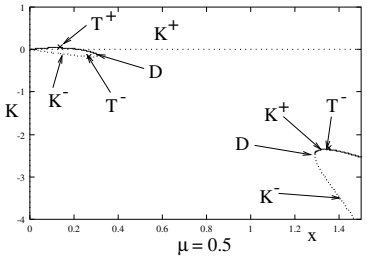

Figure 10: Solutions to (18) in the (x, K) plane for $\mu = 1/2$, $q_4 > 0$, $q_2 > 0$ and $q_3^2 > 4q_4$. See text.

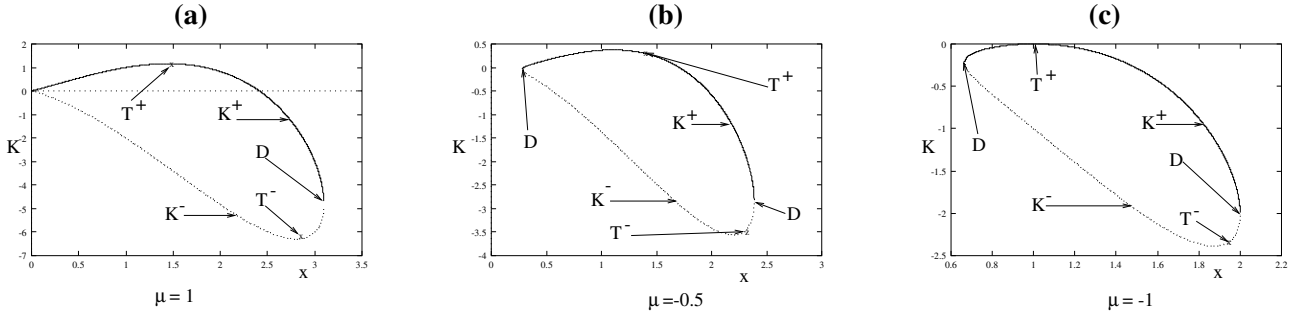

Figure 11: Solutions to (18) in the (x, K) plane for (a) $\mu = 1$ (b) $\mu = 1/2$ (c) $\mu = -1$ for $q_4 > 0$, $q_2 < 0$ and $4q_4 > q_3^2$

Homoclinic orbits are found in the same way as in the $q_4 < 0$ supercritical case. In K_+ there is a single double root between the μ-axis and T^+. Crossing T causes f to admit a dark homoclinic orbit. This persists until D at x_+, where the two sheets join. Similarly, in K_- there is a single double root until T^- is reached. Beyond T, f represents a dark homoclinic orbit. This remains until D is reached.

4.3.2 $q_3^2 > 4q_4 > 0$, supercritical

The boundary D now points down instead of up (see Figure 9 (b)). D has a maximum at $(x_m, \mu_m) = (4/5, 4/5)$. Figure 10 illustrates an $x - K$ section for constant $\mu = 0.5$, where one sees that T^+ lies in K^+ and that T^- lies in K^+ and then in K^+. $f(x)$ represents homoclinic orbits in K_+ between T^+ and D and also in the region $x > D$ and $x > T^-$.

In K_-, $f(x)$ represents homoclinic orbits in the region bounded by the origin, T^-, $x = 2q_2/(q_3^2 - 4q_4)$ and D.

4.3.3 $4q_4 > q_3^2$, subcritical

The boundary of double roots D ($\Delta = 0$) has a minimum at $(x_m, \mu_m) = (4/3, -4/3)$. Double roots exist for $0 < x_- < x < x_+$. D is a parabola that points up rather than down. The boundary passes through the origin. There are two sheets of double roots $K_\pm$. The two sheets join on D. Triple roots can exist. See Figure 12(a) for the picture. The square rooted quantity in equations (22) and (23) is defined for $x = 0$ and for $x > q_2/2q_4$. There are no quadruple roots because $x = -3q_2/8q_4$ falls outside the range for which μ is defined.

Figure 11 shows that T^+ lies in K^+ and that T^- lies in K^-. T changes sheets when it touches D

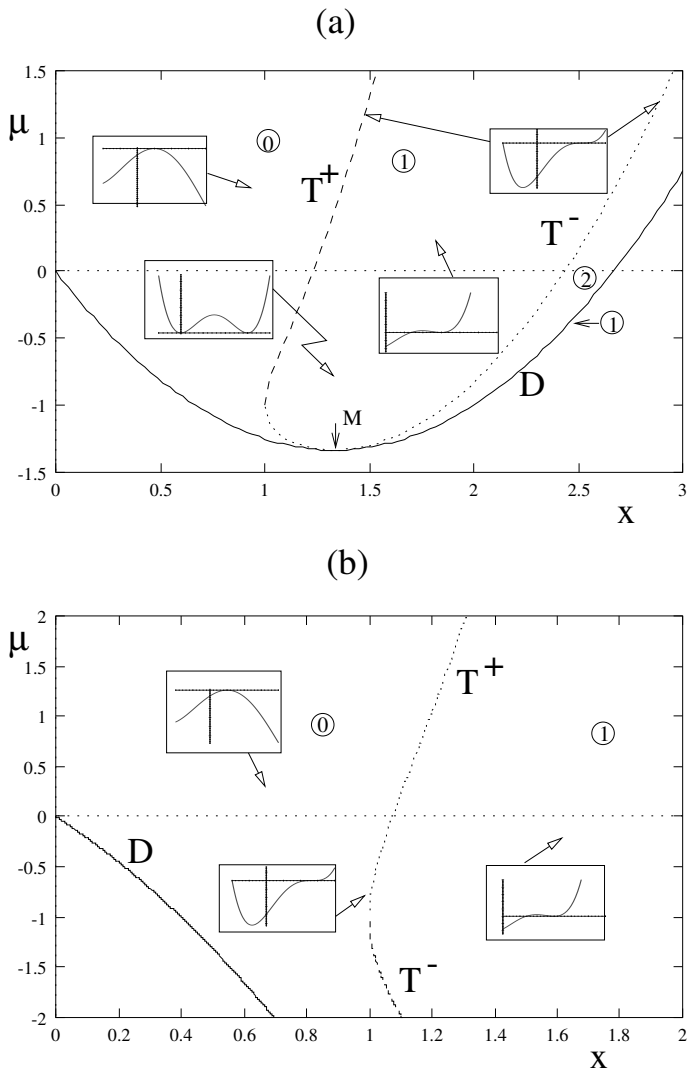

Figure 12: Projections of degenerate curves and points onto the (x, μ)-plane for $q_4 > 0$, $q_2 < 0$ and (a) $q_3^2 < 4q_4$, (b) $q_3^2 > 4q_4$. See text for details.

at (x_m, μ_m). We know that to the left of T^+ in K_+ there are simple double roots. Crossing T in K_+ causes f to represent dark homoclinic orbits. In K_- f represents simple double roots until x crosses T^-. On D $f(x_-)$ represents local maxima and $f(x_+)$ represents dark homoclinic orbits. The change occurs at x_m.

4.3.4 $q_3^2 > 4q_4 > 0$, subcritical

As we saw in the corresponding supercritical case D points down instead of up. As a result D has no turning point for $x > 0$ and so it does not touch T, see Figure 12(b). So T lies wholly in K_+ and $f(x)$ represents homoclinic orbits only in K_+ bounded by T.

4.4 Degenerate case $q_3 = 0$

There is one kind of special case, $q_3 = 0$, that affects all the cases analysed above. The degeneracy causes $K_+^2 = K_-^2$ and $H_+ = H_-$, so there are two sheets of identical solutions. Also $K_\pm = 0$ on D

($\Delta = 0$). The principal differences from $q_3 \neq 0$ in the various cases are as follows.

1. For $q_4 < 0$, $q_2 > 0$, T now forms one branch, with $f(x)$ representing double roots outside and homoclinic orbits between T and D. (see Dias & Iooss figure 5.2 for the effects of varying q_3.).

2. If $q_4 > 0$, $q_2 > 0$, T now forms a single branch with $f(x)$ having double roots between the μ-axis and T and having homoclinic orbits between T and D.

3. For $q_4 > 0$, $q_2 < 0$, T forms a single branch with $f(x)$ representing double roots between the μ-axis and T. It represents homoclinic orbits between T and D (x_+).

4.5 Summary

We have shown that there are two sheets of solutions of double roots of $f(x)$ in the (x, μ)-plane and that triple roots of $f(x)$ lie on a curve in these sheets. Let us summarise the conditions for these curves to posses homoclinic connections.

- $q_4 < 0, q_2 > 0$: a bounded curve of triple roots lies in both sheets of solutions. It together with the boundary of existence of solutions ($\Delta = 0$) enclose regions of homoclinic orbits in both sheets. The triple roots represent algebraically decaying homoclinic orbits. The quadratic curve of $\Delta = 0$ points down.

- $q_4 < 0, q_2 < 0$, there are no triple roots and no homoclinic orbits. The quadratic curve of $\Delta = 0$ points down.

- $4q_4 - q_3^2 > 0$, q_2 of either sign, there are unbounded curves of triple roots in both sheets, which together with the boundary enclose regions of dark homoclinic orbits. The triple roots do not represent homoclinic orbits. The quadratic curve of $\Delta = 0$ points up.

- $q_4 > 0, q_3^2 > 4q_4, q_2 > 0$, there is an unbounded curve of triple roots in K_+ and a small section of triple roots in K_-. So there are homoclinic orbits in both surfaces.

- $q_4 > 0, q_3^2 > 4q_4 < 0$, there is an unbounded curve of triple roots in K_+ only, so there are homoclinic orbits in K_+ only.

5 Persistence of solutions and heteroclinic tangles

So far we have considered only solutions of the normal form equations (7), (8) with $R_A = R_B = 0$. The question of persistence of solutions under the addition of remainder terms that break the completely integrable structure of the normal form is more delicate. We shall only consider this question for solutions (either homoclinic or heteroclinic) that lie in the unstable manifold of the origin $W^u(0)$ for $\mu < 0$. Then, since the origin is a saddle-focus, $W^u(0)$ is two-dimensional and transverse intersections between $W^u(0)$ and the symmetric section $\mathcal{S}$ will survive under small perturbations. Such solutions will be symmetric homoclinic orbits.

Now, for subcritical bifurcations away from the codimension-two point, i.e. when $q_2 < 0$ is not small, we have the bifurcation for $\mu < 0$ of a one-parameter family (14) of homoclinic orbits of the truncated normal form (7), (8). A careful argument in Iooss & Pérouème (1993) shows that when remainder terms are included that break the completely integrable structure of the normal form, the two solutions with phases $\phi = 0$ and π correspond to symmetric solutions and they do indeed persist for μ sufficiently small. In fact, if we can prove that these two orbits are transverse, then the analysis of (Härterich 1998) for reversible systems or Devaney (1976*a*) for Hamiltonian systems will additionally give infinitely many *N-pulse* orbits (homoclinic solutions which resemble N copies of the primary placed end to end) for each N and each small μ, although none of them bifurcates from $\mu = 0$. Indeed, an intricate bifurcation

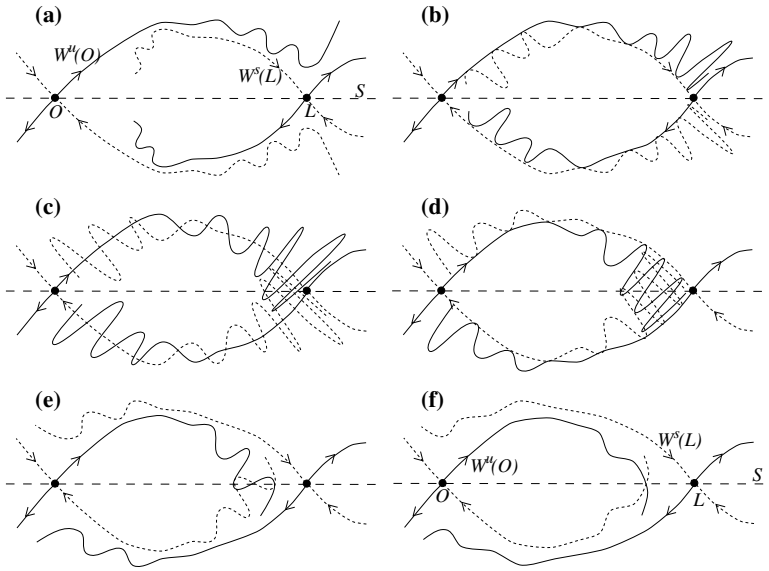

Figure 13: Illustrating the parameter unfolding of two successive heteroclinic tangencies between a saddle-focus equilibrium O and a saddle-type periodic orbit L for a four-dimensional reversible Hamiltonian system. The picture is drawn schematically by taking a formal Poincaré section within the zero level set of the Hamiltonian function, $\mathcal{S}$ is the symmetric section, and unstable and stable manifolds are depicted respectively by solid and broken lines. Each point at which $W^u(0)$ intersects $\mathcal{S}$ corresponds to a symmetric homoclinic orbit. For the unfolding of the normal form, panels (a)–(f) correspond to increasing μ through the critical value $\mu_D = -\frac{3q_2^2}{16q_1q_4}$ for $q_4 > 0$ and $q_2 < 0$.

picutre of multi-pulse solutions has been found both numerically (Buffoni, Champneys & Toland 1996) and asymptotically (Yang & Akylas 1997) for equation (3) with $b = 0$.

Also, for $\mu = 0$ Iooss (1997) has shown the persistence of the two symmetric algebraically decaying solitary waves (limits of (15) as $\mu \to 0$, see Figure 3) for $q_4 < 0$ and $q_2 > 0$ small.

We now turn our attention to the heteroclinic connections that occur along the curve $\mu = \mu_D$ for $q_4 > 0$ and $q_2 < 0$ (see Figure 2). Recall that these correspond to heteroclinic connections from the origin to the small-amplitude periodic solution represented by the non-trivial double root of $f(|A|^2)$. Putting back in the arbitrary phase ϕ, we have a one-parameter family of such heteroclinic connections. When normal-form breaking remainder terms are added, such a family of heteroclinic connections is structurally unstable because it involves the identification of two-dimensional stable and unstable manifolds of the origin and the periodic orbit. A Melnikov-type analysis would need to be performed in order to judge how this highly degenerate situation unfolds upon addition of remainder terms R_A and R_B. Such an analysis is likely to be highly involved and be sensitively dependent on the form of the remainders, and we do not attempt to perform it here. Instead we merely state that one of the simplest generic unfoldings is that the degenerate heteroclinic family breaks up into a pair of heteroclinic tangencies occuring at nearby μ-values.

Figure 13 shows how such a bifurcation sequence would unfold for reversible Hamiltonian systems. The dynamics are clearly highly complex, but we remark only how the the unfolding the leads to infinitely many symmetric *homoclinic* orbits (intersections between $W^u(0)$ and the symmetric section $\mathcal{S}$). Each successive homoclinic solution has one more oscillation near the periodic orbit L. Carefully tracing how the infinitely many homoclinic orbits in panel (d) of Figure 13 are created as the parameter varies, we find that all the solutions lie on a single curve in a bifurcation diagram. This curve snakes to and fro, involving successive folds as the solution generates more and more bumps (oscillations close to the periodic orbit). See Figure 14 below for a numerically computed curve and Hunt, Lord & Champneys (1998, Sect. 4) for a more detailed justification of the construction in Figure 13 and why it leads to such a snaking curve. Finally, since there are two primary solutions which bifurcate from

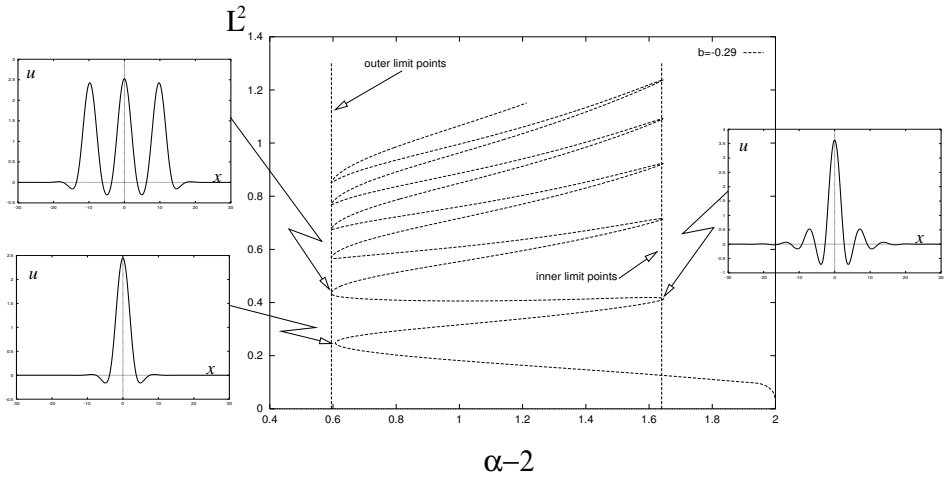

Figure 14: Continuation in P of the primary homoclinic orbit from the reversible-Hopf bifurcation at $P = 2$ of (3) with $b = 0.29$.

$\mu = 0$, we should expect to see this snaking curve repeated for each of the two primaries (see Figure 16 below).

Let us reiterate that we have not proved anything, we have merely constructed a simple possible unfolding of the degenerate heteroclinic connection in the normal form. As we shall now see though, this unfolding is bourn out in numerical experiments on the example equation (3).

6 Numerical results

With the aid of Maple program derived from Kuznetsov (1995, Ex.15, §8.7) we have calculated the important normal form coefficients for (3) (see Woods (1998) for the details). Specifically we get

$$\mu = P - 2 \tag{25}$$

$$q_1 = 1/4 \tag{26}$$

$$q_2 = -\frac{19}{18}a^2 + \frac{3}{4}b \tag{27}$$

$$q_4 = \frac{12007}{576}a^2 b - \frac{687295}{46656}a^4 - \frac{327}{512}b^2. \tag{28}$$

So q_2 changes sign at $b = 38a^2/27$ and at this value q_4 is positive.

6.1 Homoclinic snaking

In what follows we shall compute bifurcation curves of homoclinic and heteroclinic orbits to (3) as P and b vary, holding a fixed at 1. Note that, provided it is non-zero, a can be scaled out of the equation by the transformation $\tilde{u} = au$ hence there is no loss of generality. All computations are performed using the numerical continuation software AUTO (Doedel, Champneys, Fairgrieve, Kuznetsov, Sandstede & Wang 1997). Figure 14 shows the bifurcation diagram, for the typical value $b = 0.29$ (but note this is a long way from $38/27$ where $q_2 = 0$), of the simplest symmetric homoclinic orbit which emanates from the Hamiltonian-Hopf bifurcation point at $P = 2$. The ordinate of this and subsequent bifurcation diagrams is a constant multiple of the vector L^2-norm of $(u(t), u'(t), u''(t), u'''(t))$. At each successive pair of limit points of the curve, the homoclinic solution gains an extra pair of 'bumps' close to the periodic solution. The insets in the figure show this process for the first 3 folds. As the curve climbs in L_2-norm the process repeats, creating a homoclinic solution with arbitrarily large norm and arbitrarily many large-amplitude bumps. Notice how the successive limit points converge rapidly to two distinct

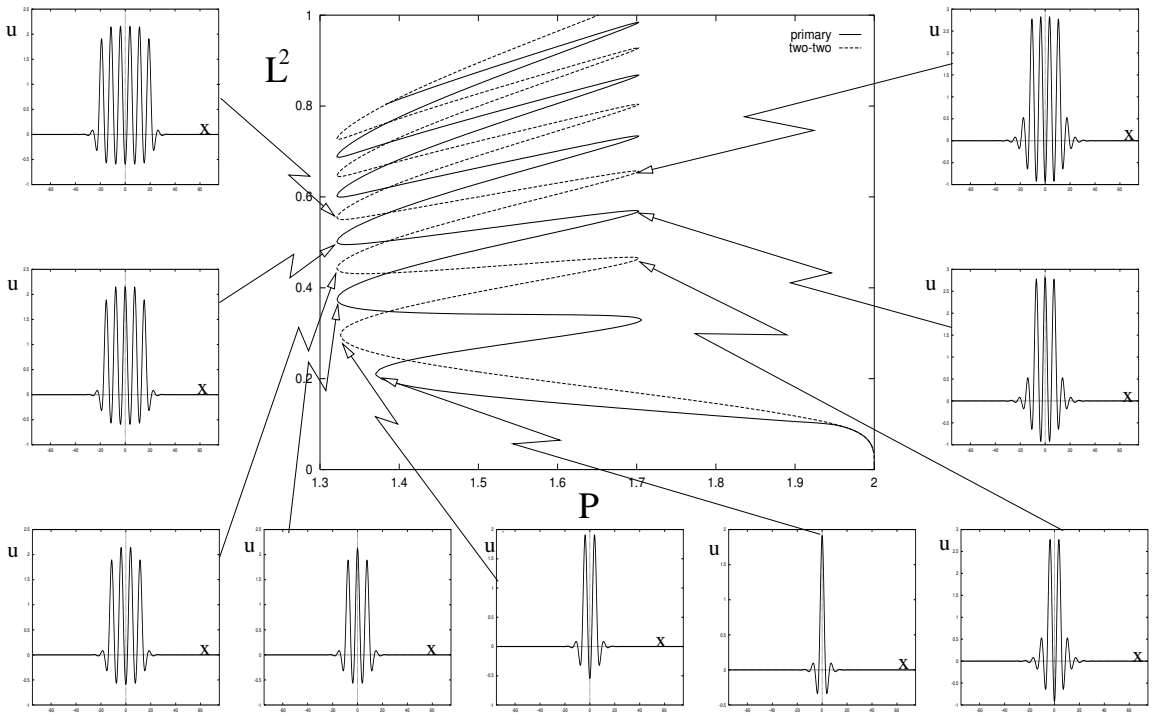

Figure 15: Continuation in P for $b = 0.3$ showing the formation of multi-pulse solutions for both the primary and the **2**(2) branch

P-values. These parameter values correspond to those at which the heteroclinic tangencies of Figure 13 occur. Moreover, these numerics agree with the theoretical prediction (Hunt, Lord & Champneys 1998, sect. 4) that if the periodic orbit L has positive Floquet multipliers, then the limit points should converge to the two heteroclinic-tangency parameter values from the right.

Figures 15 and 16 show similar figures for two different b-values, one further away and one closer to the codimension-two point $b = 38/27$. In both figures, we have also computed the other branch of homoclinic solutions that bifurcates from $P = 2$ (in the notation of Buffoni, Champneys & Toland (1996) this is the **2**(2) branch). Note how the bifurcation branches of these two homoclinic orbits become intertwined. The primary creates solutions with odd numbers of bumps close to the periodic orbit and the **2**(2) creates homoclinic solutions with even numbers of bumps. As b is decreased towards $38/27$, the value at which $q_2 = 0$ for (3), the oscillations in P decrease in amplitude (see Figure 16).

Figure 17 shows the distribution of limit points as μ and q_2 are varied for (3). The two numerical curves of limit points were taken on the primary branch after sufficiently many wiggles to be close to the two μ-values at which the limit points converge (the two heteroclinic tangencies). Notice from Figure 17(b) how the numerical and theoretical curves appear to agree in the limit $P \to 2$. For P small, the normal form curve lies approximately between the two numerical curves of limit points. However, note how rapidly the two heteroclinic tangencies contract onto the normal form curve as $P \to 2$. This suggests that the unfolding of the degenerate bifurcation curve is a 'beyond all orders' effect, as is usual in breaking structurally unstable curves of normal forms.

6.2 Kinks – a degenerate bifurcation diagram

For $b = 0$, it is known (partially analytically, partially numerically) that the primary branch born in the reversible-Hopf bifurcation at $P = 2$ can be traced all the way back to $P = -\infty$, including passing through the 'node focus transition' of the origin at $P = -2$ (see Buffoni, Champneys & Toland (1996) and references therein). Thus a gross transition must take place in the bifurcation diagram between $b = 38/27$ and $b = 0$, as partially summarised in Figure 18. In fact, the transition occurs at precisely

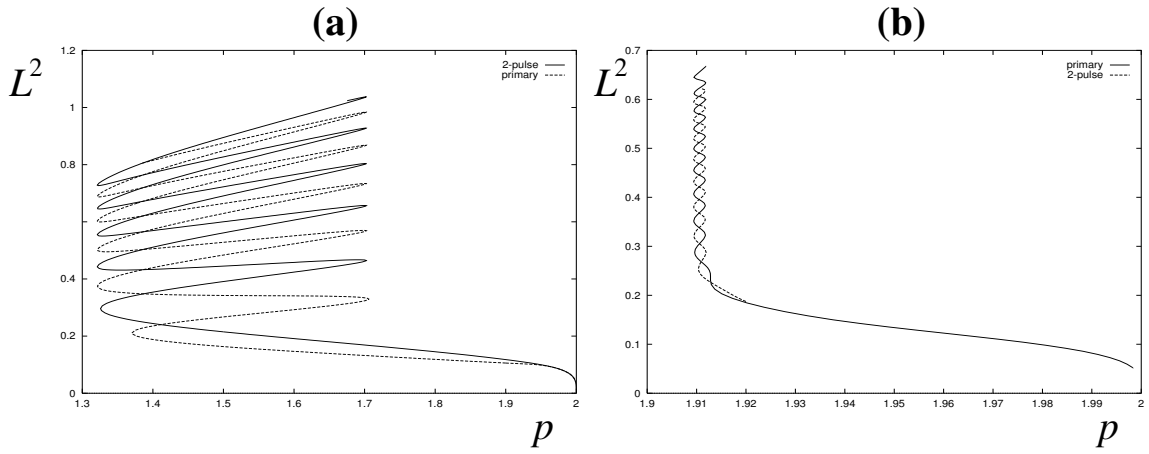

Figure 16: Indicating how the width of the snaking decreases rapidly as b increases; (a) $b = 0.3$ and (b) $b = 0.594$.

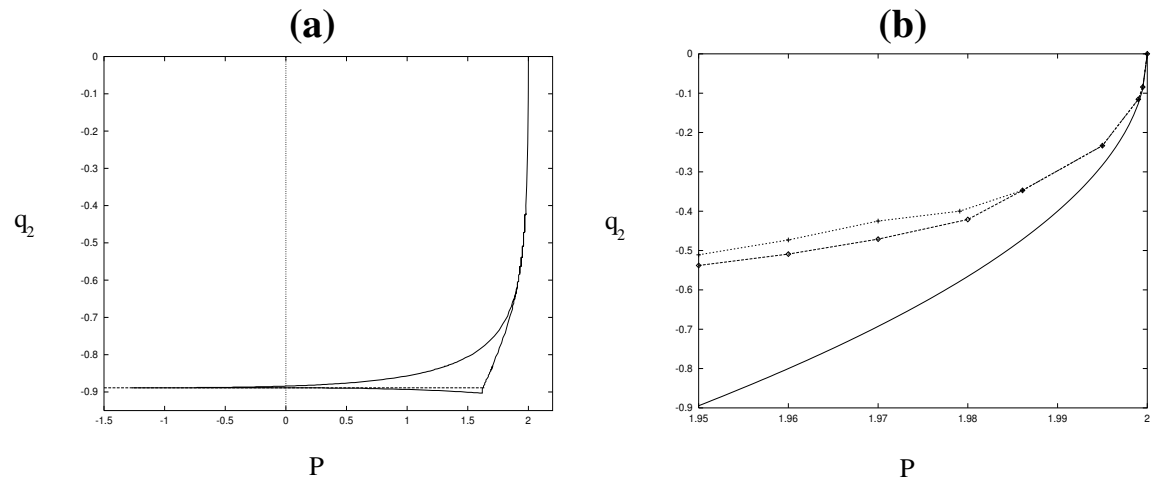

Figure 17: (a) The results of two-parameter continuation in P and b of an inner and outer limit point (with respect to P) of the primary homoclinic orbit. The dashed line corresponds to the kink solution for $b = \frac{2}{9}$ (see Section 6.2) (b) A comparison with normal form theory near $(P, q_2) = (2, 0)$. The line represents the normal-form calculation of the heteroclinic connection using (25)–(28). The points represent numerically calculated curves of limit points.

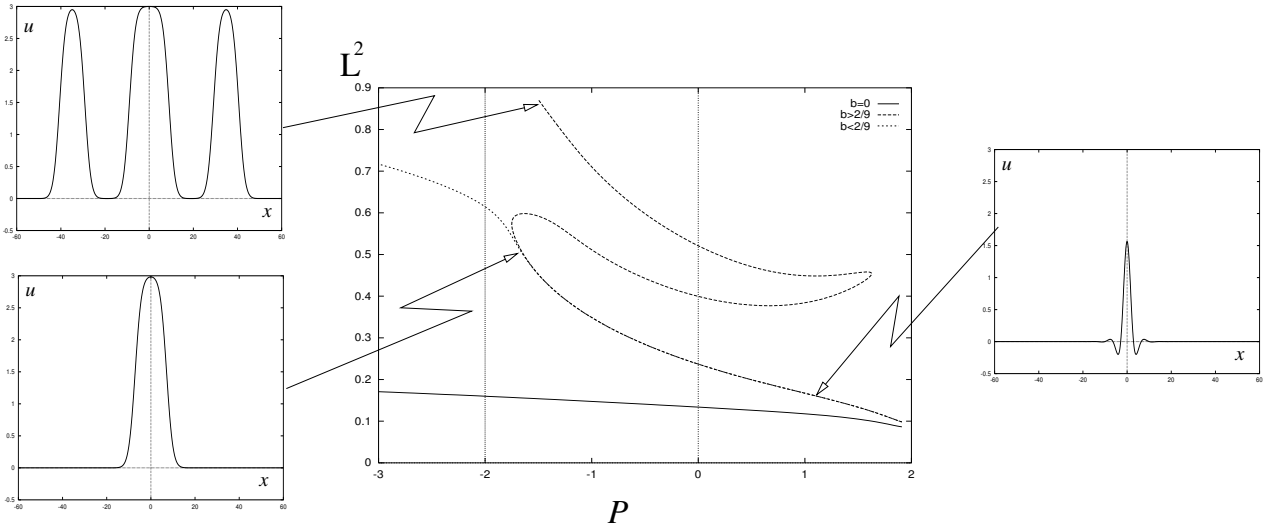

Figure 18: Continuation in P of the one-bump solution starting at the reversible Hopf for $b = 0$, $b = (2/9)^-$, and $b = (2/9)^+$. The insets indicate that as the transition $b = 2/9$ is approached the orbits on the snaking bifurcation curve approach multi-pulse version of a 'kink' connection between $u = 0$ and $u = 3$.

$b = 2/9$, at which value there is a non-trivial equilibrium at $u = 3$ that has exactly the same value of the Hamiltonian ($H = 0$) as the origin (cf. Eqns. (4) and (6)). Therefore, precisely for this b-value alone, there is the possibility of heteroclinic connections between $u = 0$ and $u = 3$. In the parlance for pattern formation, we shall refer to such solutions as *kinks*. It turns out that such kinks do exist, as may be inferred from the analysis of the so-called extended Fisher-Kolmogorov (EFK) equation to which (3) with $b = 2/9$ may be transformed by $u \to u - 1.5$ and scaling parameters and variables. Moreover, the existence of kinks for this unique b-value plays an incisive role which we now describe.

As b is decreased from $b = 38/27$ towards $b = 2/9$, the snaking of the primary branch widens towards $P = -2$. In so-doing the amplitude of the periodic solution to which heteroclinic connections are made increases. Until, at $b = 2/9$, the periodic orbit forms itself into the kink. After the kink is destroyed, i.e. for $b = (2/9)^-$, then suddenly a whole new branch of primary solutions has been created (from infinity in the L_2 norm) stretching from $P = -2$ back towards $P = -\infty$. These solutions are like small perturbations from a branch of kink solutions that exist only at $b = 2/9$. Such a branch has been computed numerically and is presented in Figure 19.

Numerically we find that the kink can be traced back from $P = -\infty$, and passes through $P = -2$ where the eigenvalues of *both* the origin and $u = 3$ become complex (a node-focus transition). Note that the linearisation around the two equilibria is identical, since for $b = 2/9$, equation (3) is invariant under the transformation $\tilde{u} = 3 - u$, which maps the two equilibria into one another. Moreover, owing to this symmetry all kinks computed in Figure 19 are odd in $u - 1.5$. Hence the kinks develop decaying oscillations in their tails as they pass through $P = -2$. At $P \approx 1.645$ the kink turns around at a limit point in its bifurcation diagram and returns towards $P = -2$ as a three-transition kink solution. From theoretical considerations we strongly suspect that such a solution survives back to $P = -2$ where the six layers of near constant $u = 0$ or $u = 3$ become infinitely wide. However, there are numerical difficulties in computing towards this limiting P-value.

Finally we note that the kink solutions in Figure 19 are only two of an infinite family that appear to exist for all $P \in (-2, 2)$ when $b = 2/9$. Figures 20 and 21 shows a bifurcation diagram of a sample of extra multi-layered kinks. Again, for theoretical reasons we expect that other than the primary kink solution, all others terminate at the node-focus transition $P = -2$ by the transition layers becoming infinitely wide as $P \to -2$.

Note that the overall bifurcation behaviour is remarkably similar to that known to occur for *homoclinic* solutions of (3) for $b = 0$ (Buffoni, Champneys & Toland 1996).

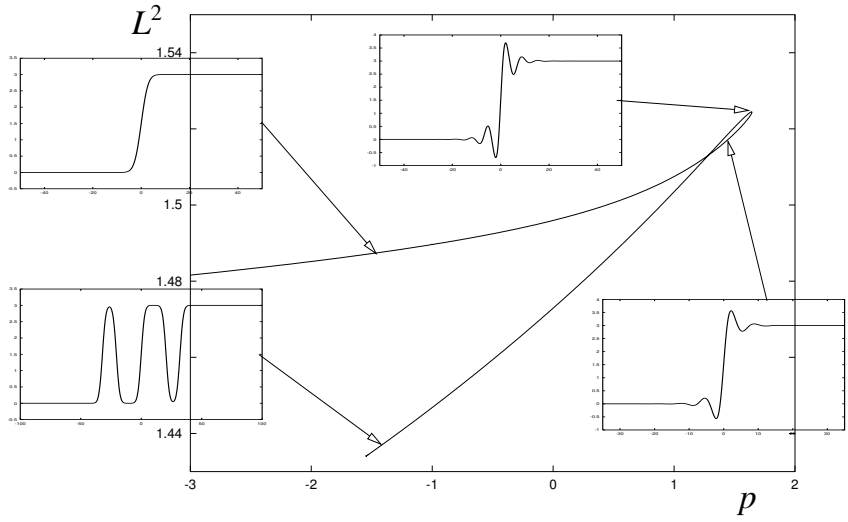

Figure 19: Kink solutions for $b = 2/9$

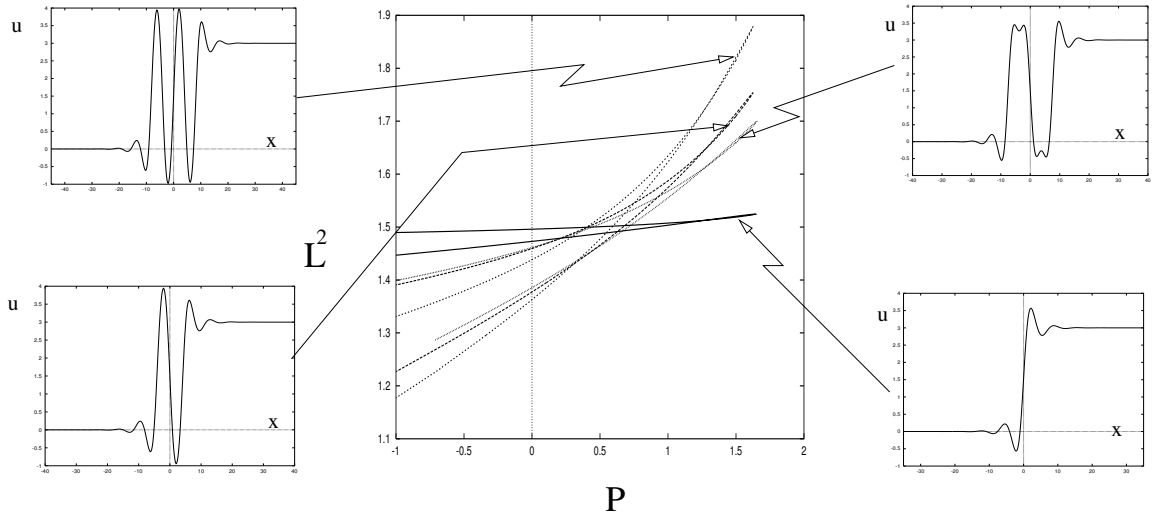

Figure 20: Multi-kink solutions for $b = 2/9$

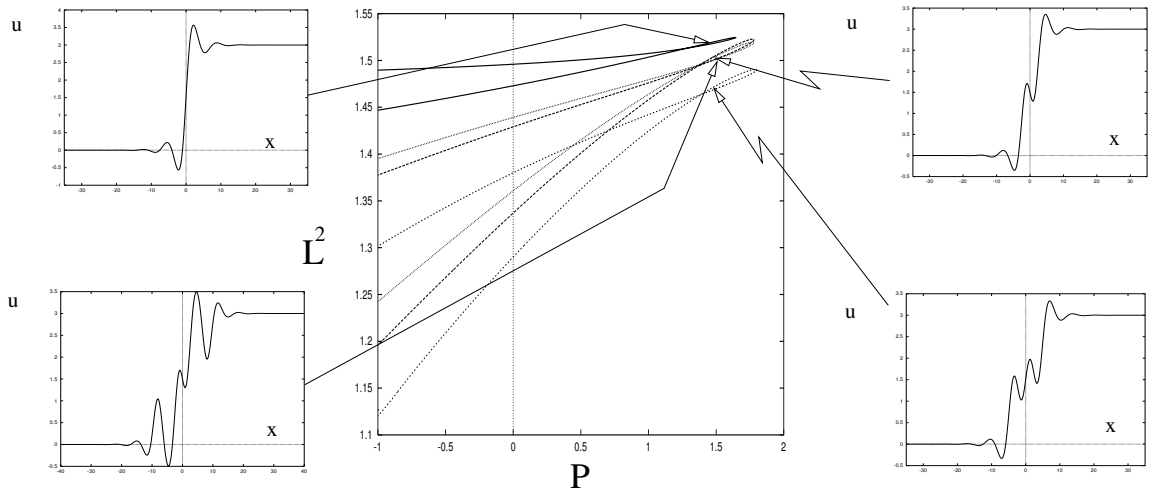

Figure 21: Other complex kink solutions for $b = 2/9$

7 Discussion

The analysis is this paper has been somewhat heuristic, since we have not treated with any rigour the question of persistence of solutions to the truncated normal form equations. Nevertheless, the geometric analysis based only on studying the graph of the potential f does seem to provide insights which are fully bourn out in accurate numerical experiments on an example system. We also have no reason to believe that the example is in any way special among the class of systems undergoing the degenerate reversible Hamiltonian Hopf bifurcation described in this paper. In fact, in a sister paper to this one (Hunt, Woods, Champneys, Peletier, Wadee & Budd 1998), several systems arising from structural mechanics are reviewed which all appear to possess the snaking of homoclinic solutions as embodied in Figures 14 and 15. Included in these examples is the model of an axially-compressed cylindrical shell, which is governed by a coupled system of fourth-order elliptic PDEs (see Hunt, Lord & Champneys (1998)). So it would seem that even our numerical extensions to what the normal form calculations suggest may well be ubiquitous.

There are of course, certain necessary hypotheses that must be satisfied in order for a system to undergo the sequence of bifurcations described above. For equations of the form (3), for example, note that there have to be at least two nonlinear terms for the existence of degenerate Hamiltonian-Hopf bifurcations and kink solutions connecting to the origin. An easy way to see this is that the coefficient of a single nonlinearity may be scaled away via a coordinate change. Also we have looked at kinks with the linearisation $u_{tttt}+Pu_{tt}+u=0$, however a simple scaling results in a linearisation $u_{tttt}+u_{tt}+cu=0$, which arises as the travelling wave equation for solutions of the 5th-order KdV equation. Hence, this offers the possibility that similar dynamics to that described here, may be found for travelling wave problems arising from higher-order and coupled KdV-type systems (e.g. Kichenassamy & Olver (1996), Gottwald, Grimshaw & Malomed (1997)). We also note the existence of kink-like numerical solutions of an exact formulation for interfacial water waves in the work of Turner & Vanden-Broek (1988). In their problem a homoclinic orbit is continued from small amplitude until it broadens and begins to look like a kink. The orbit's amplitude and wave speed approach limiting values.

Numerical experiments presented in Section 6 above revealed a complex bifurcation scenario involving (for $b=2/9$) a heteroclinic connection between the origin and a nontrivial equilibrium. Work in progress is currently directed towards proving some rigorous statements about the existence of some of these solutions. For example it is known (Amick & Toland 1992, Buffoni, Champneys & Toland 1996) that when $b=0$ there is a unique homoclinic solution for all $P<-2$ and that this bifurcates into infinitely many multi-pulse solutions for $P>-2$. It is natural to conjecture that these properties remain true for all $b\in[0,2/9)$. Moreover one might conjecture that the unique homoclinic orbit for $b<2/9$, $P<-2$ forms a continuous branch with the kink solution that exists for $b=2/9$ $P<-2$, and that there are no homoclinic solutions to the origin for $b>2/9$, $P<-2$. The shooting methods used by Amick & Toland (1992) may prove useful in proving these conjectures. See also van den Berg (1997) for an application of these methods for showing existence and uniqueness of heteroclinic connections for the EFK equation. Recall that for $b=2/9$, letting $u\to u-1.5$, we recover the EFK equation, which is just a scaling of Equation (3) with $a=0$, for which much information is already know rigorously concerning the existence of kinks (Kalies & Vandervorst 1996, Peletier & Troy 1996).

References

Amick, C. & Toland, J. (1992), 'Homoclinic orbits in the dynamic phase-space analogy of an elastic strut', *European J. Appl. Mech.* **3**, 97–114.

Buffoni, B. & Séré, E. (1996), 'A global condition for quasi-random behaviour in a class of conservative systems', *Commun, Pure Appl. Math.* **49**, 285–305.

Buffoni, B., Champneys, A. & Toland, J. (1996), 'Bifurcation and coalescence of a plethora of homoclinic orbits for a Hamiltonian system', *J. Dyn. Diff. Eqns.* **8**, 221–281.

Buffoni, B., Groves, M. & Toland, J. (1996), 'A plethora of solitary gravity-capillary water waves with nearly critical bond and froude numbers.', *Phil. Trans. Roy. Soc. Lond. A* **354**, 575–607.

Champneys, A. R. (1998), 'Homoclinic orbits in reversible systems and their applications in mechanics, fluids and optics', *Physica D* **112**, 158–186.

Devaney, R. (1976*a*), 'Homoclinic orbits in hamiltonian systems', *Journal of Differential Equations* **21**, 431–438.

Devaney, R. (1976*b*), 'Reversible diffeomorphisms and flows', *Trans. Amer. Math. Soc.* **218**, 89–113.

Dias, F. & Iooss, G. (1996), 'Capillary-gravity interfacial waves in infinite depth', *Eur.J.Mech.,B/Fluids* **15**(3), 367–393.

Doedel, E., Champneys, A., Fairgrieve, T., Kuznetsov, Y., Sandstede, B. & Wang, X. (1997), 'AUTO97 continuation and bifurcation software for ordinary differential equations'.

Elphick, C., Tirapegui, E., Brachet, M., Coullet, P. & Iooss, G. (1987), 'A simple global characterization for normal forms of singular vector fields', *Physica D* **29**, 95–127.

Glebsky, L. & Lerman, L. (1995), 'On small stationary localized solutions for the generalized 1-d swift-hohenburg equation', *Chaos* **5**(2), 424–431.

Gottwald, G., Grimshaw, R. & Malomed, B. (1997), 'Parametric envelope solitons in coupled korteweg-de vries equations', *Physics Letters A* **227**, 47–54.

Härterich, J. (1998), 'Cascades of reversible homoclinic orbits to a saddle-focus equilibrium', *Physica D* **112**, 187–200.

Hilali, M., Métens, S., Borckmans, P. & Dewel, G. (n.d.), 'Pattern selection in the generalized swift-hohenburg model'.

Hunt, G. & Wadee, M. (1991), 'Comparative Lagrangian formulations for localised buckling', *Proc. R. Soc. Lond. A* **434**, 485–502.

Hunt, G., Bolt, H. & Thompson, J. (1989), 'Structural localization phenomena and the dynamical phase-space analogy', *Proc. R. Soc. Lond.* **A 425**, 245–267.

Hunt, G., Lord, G. & Champneys, A. (1998), 'Homoclinic and heteroclinic orbits underlying the post-buckling of axially-compressed cylindrical shells'. to appear in *Computer Methods in Applied Mechanics and Engineering* theme issue on 'Computational Methods and Bifurcation Theory with Applications'.

Hunt, G., Woods, P., Champneys, A., Peletier, M., Wadee, M. & Budd, C. (1998), 'Compartmental buckling in long structures'. In preparation.

Iooss, G. (1997), 'Existence d'orbites homoclines á un équilibre elliptique pour un système réversible', *C. R. Acad. Sci. Paris, Ser. 1* **324**, 993–997.

Iooss, G. & Kirchgässner, K. (1990), 'Bifurcation d'ondes solitaires en présence d'une faible tension superficielle', *C. R. Acad. Sci. Paris, Ser. 1* **311**, 265 –268.

Iooss, G. & Pérouème, M. (1993), 'Perturbed homoclinic solutions in reversible 1:1 resonance vector fields', *Journal of Differential Equations* **102**, 62–88.

Kalies, W. & Vandervorst, R. (1996), 'Multitransition homoclinic and heteroclinic solutions of the extended Fisher-kolmogorov equation', *J. Diff. Eqns.* **131**, 209–228.

Kichenassamy, S. & Olver, P. (1996), 'Existence and non-existence of solitary wave solutions to higher-order model evolution equations', *SIAM J. Math. Anal.* **23**, 1141–1166.

Kuznetsov, Y. (1995), *Applied bifurcation Theory*, Springer-Verlag.

Lamb, J. & Roberts, J. (1998), 'Time-reversal symmetry in dynamical systems: A survey', *Physica D* **112**, 1–39.

Peletier, L. & Troy, W. (1996), 'A topological shooting method and the existence of kinks of the Extended Fisher-Kolmogorov equation', *Topological Methods in Nonlinear Analysis* **6**, 331–355.

Turner, R. & Vanden-Broek, J.-M. (1988), 'Broadening of interfacial solitary waves', *Physics of Fluids* **31**(9), 2486–2490.

van den Berg, J. (1997), 'Uniqueness of solutios for the extended fisher-kolmogorov equation'. Report W 97-24, Mathematics Institute, University of Leiden.

van der Meer, J. (1985), *The Hamiltonian Hopf bifurcation*, Lecture Notes in Mathematics 1160, Springer-Verlag, Berlin.

Woods, P. (1998), Localized buckling and 4th-order equations, PhD thesis, University of Bristol.

Yang, T.-S. & Akylas, T. (1997), 'On asymmetric gravity-capillary solitary waves', *J. Fluid Mech* **330**, 215–232.